Single-crystal growth and investigation of Na_xCoO_2 and $Na_xCoO_2 \cdot yH_2O$

D. P. Chen, H. C. Chen, A. Maljuk, A. Kulakov, H. Zhang, P. Lemmens, and C. T. Lin*
Max Planck Institute for Solid State Research, Heisenbergstrasse 1, D-70569 Stuttgart, Germany
(Received 12 January 2004; revised manuscript received 22 March 2004; published 15 July 2004)

A systematic study of Na_xCoO_2 ($x=0.50-0.90$) and $Na_xCoO_2 \cdot yH(D)_2O$ ($x=0.26-0.42$, $y=1.3$) has been performed to determine phase stability and the effect of hydration on the structural and superconducting properties of this system. We show that a careful control of the Na deintercalation process and hydration dynamics is possible in single crystals of this system. Furthermore, we give experimental evidence that the dependence of the superconducting transition temperature on Na content is much weaker than reported earlier. Implications of this effect for the understanding of the superconducting phase diagram are discussed.

DOI: 10.1103/PhysRevB.70.024506 PACS number(s): 74.62.Bf, 61.10.−i, 74.25.Dw

I. INTRODUCTION

The recently discovered superconductor $Na_xCoO_2 \cdot yH_2O$ has attracted considerable attention as being the first superconducting cobaltite, and as evidence that important electronic correlations exist.[1] Its superconducting transition temperature of maximum $T_c \approx 5$ K exhibits a composition dependence, decreasing for both underdoped and overdoped materials, as observed in the cuprates. This suggests that a detailed characterization of the electronic and magnetic behavior of this new type of materials and their interplay with structural peculiarities may contribute to a more fundamental understanding of the high T_c superconductivity in cuprates, such as the layered crystal structure,[2] magnetic susceptibility,[3,4] electronic anisotropy,[5] irreversibility lines, and superconducting parameters λ_{ab}, H_{c2}.

The physical properties are determined by the amount of sodium and water in $Na_xCoO_2 \cdot yH_2O$ via their influence on the Co valence state and the resulting local distortions of the CoO_6 octahedra present in the structure. The compound Na_xCoO_2 shows manifestations of frustration in its physical properties because Co occupies a triangular lattice and the exchange interactions are antiferromagnetic.[6,7] The close relationship between structural and electronic properties establishes itself also on the Fermi surface that is expected to show features of strong nesting.[8,9] Furthermore, there exists evidence that superconductivity might have an unconventional order parameter.[8] When water is introduced into the compound, it exhibits chemical and structural instabilities. The Na^+ ions are at least partially mobile at elevated temperatures and may order at low temperatures in dependence of composition and sample treatment. The same is proposed for the Co^{4+}/Co^{3+} charge state on the triangular lattice.[10]

All of these features make the study of the physical and chemical properties of the compounds difficult. However, nearly all the studies reported so far have been made on either sintered specimens or poorly characterized polycrystalline samples. These materials are often found to be inhomogeneous, especially with respect to the distribution of Na^+ ions in the lattice and in the intergranular spaces, the Na_2O decomposition of the compound, and with respect to the intercalation of water. In polycrystalline samples water may in part accumulate in intergranular spaces. The possible presence of second phases leaves a degree of uncertainty when interpreting the structure and the electrical and superconducting properties as function of composition, i.e., establishing a superconducting phase diagram. This problem may be circumvented by the use of high quality single crystals whose chemical composition and crystal structure can be properly determined.

When growing Na_xCoO_2 single crystals, considerable difficulties appear on account of the high Na_2O vapor pressure, which increases exponentially from 10^{-5} to 10^{-3} Torr with heating to temperatures between 500 and 800 °C, followed by a noticeable evaporation. Therefore ceramic powders were synthesized using additional Na_2CoO_3 for compensation of the Na loss during heating[2,11] or a "rapid heat-up" technique[12] to avoid the formation of a nonstoichiometric compound. Solution growth by using NaCl flux[13] was performed that unfortunately lead only to thin crystals (<0.03 mm) or nonstoichiometric and possibly contaminated samples. To obtain the superconducting phase the crystal must be hydrated by chemical oxidation.[1] The compound can be partially decomposed during the oxidation process, leading to highly defective crystals containing Na-poor phases.

In this contribution we present a single crystal growth method to prepare large and high quality single crystals and demonstrate their chemical, thermal, and structural behavior and electric properties under dry and humid conditions.

II. EXPERIMENT

Single crystals were grown in an optical floating zone furnace (Crystal System Incorporation, Japan) with 4×300 W halogen lamps installed as infrared radiation sources. Starting feed and seed materials were prepared from Na_2Co_3 and Co_3O_4 of 99.9% purity with the nominal composition of Na_xCoO_2, where $x=0.50$, 0.60, 0.70, 0.75, 0.80, 0.85, and 0.90, respectively. Well-mixed powders were loaded into alumina crucibles and heated at 750 °C for a day. The heated powders were reground and calcined at 850 °C for another day. They were then shaped into cylindrical bars of $\approx 6 \times 100$ mm by pressing at an isostatic pressure of ≈ 70 Mpa and then sintered at 850 °C for 1 day in flowing oxygen to form feed rods.

The sintered feed rod was premelted with a mirror scanning velocity of 27 mm/h by traveling the upper and lower shafts, respectively, to densify the feed rod. After premelting the ≈20 mm long rod was cut and used as a first seed and hereafter the grown crystal was used as a seed. The feed rod and the growing crystal were rotated at 15 rpm in opposite directions. In an attempt to reduce the volatilization of Na and obtain stoichiometric and large crystals, we applied traveling rates of 2 mm/h under pure oxygen flow of 200 ml/min throughout the growing procedure.

To obtain superconductivity the Na was partly extracted by placing crystals in a 6.6 mol Br_2/CH_3CN solution for 100 h and then washed out by H_2O or D_2O solution.[1] Alternatively, the electrochemical technique was also applied, using an aqueous solution of NaOH as an electrolyte to partially extract Na.[14] This technique needs a longer time for deintercalation and the resulting superconducting transitions are generally sharper.

Thermogravimetric and differential thermal analysis (TG-DTA) was performed to study the melting behavior as well as the time and temperature dependence of the water loss in the compound. Single crystal XRD measurements were carried out with the x-ray diffractometer (Philips PW 1710) using Cu $K\alpha$ radiation, a scanning rate of 0.02° per second, and θ–2θ scans from 5° to 90°. The lattice parameters obtained from XRD data were refined using the commercial program PowderCell. The chemical composition was determined by energy dispersive x ray (EDX) including microanalysis. The as-grown crystals were cleaved parallel to the a axis and the composition of Na and Co was determined across the cleaved section.

III. RESULTS AND DISCUSSIONS

A. DTA-TG analysis

The melting behavior of a $Na_{0.7}CoO_2$ crystal was investigated by DTA-TG measurements and with a high temperature optical microscope. A small single crystal was loaded in a Pt crucible and then heated in the DTA-TG apparatus (NETZSCH STA-449C) at 7.5 °C/min up to 1200–1250 °C in flowing oxygen. Two peaks with onset $T_1 = 1035$ °C and $T_2 = 1092$ °C on the DTA curve correlate very well with a weight loss observed by TG, as shown in Figs. 1(a) and 1(b), respectively. No weight changes were observed below 980 °C.

The high temperature optical microscope study of the crystal reveals that the liquid phase appears at $T_1 = 1035$ °C but the solid phase (crystal) still remains up to $T_2 = 1092$ °C, exhibiting a coexistence of solid and liquid phases. Our investigations indicate that thermal decomposition of $Na_{0.7}CoO_2$ is accompanied by a weight loss down to 96.2 wt% and the compound decomposes into a sodium-rich liquid and a cobalt-rich solid phase,[15,16] assuming chemical reaction of the melt as follows: $Na_xCoO_2 -> CoO + \text{liquid (Na-rich)} + xO_2 - (T > 1100\,°C) -> [Na_xCoO_{1.65}]^*$ (* = homogeneous melt).

The dissolution of CoO occurs in the Na-rich melt and by taking up oxygen from the environment. Thus it results in an increase of weight because the oxidation state of cobalt is significantly higher in the melt, i.e., $Co^{+2.7}$, according to the chemical reaction equation shown above. A sharp weight loss down to 95.5 wt% occurs at $T_2 = 1092$ °C and the melt starts to get homogeneous and stable. A nearly constant weight of 95.5–94.9 wt% is obtained in the temperature range of 1120–1200 °C, where the melt becomes homogeneous. A monotonic weight loss of melt may happen under constant heating. Evidently, the melting behavior described so far indicates that the compound melts incongruently.

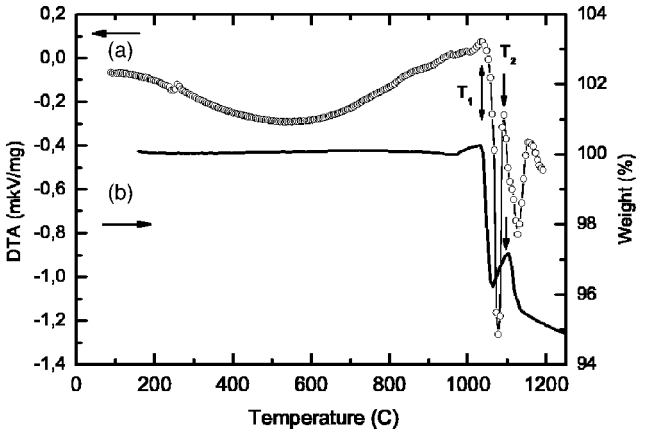

FIG. 1. DTA-TG analysis by melting single crystalline $Na_{0.7}CoO_2$ heated at 7.5 °C/min up to 1200–1250 °C in flowing oxygen. $T_1 = 1035$ °C, $T_2 = 1092$ °C. (a) The melting behavior of the compound, and (b) temperature dependence of the weight loss.

B. Crystal growth, morphology and composition

When sintering Na_xCoO_2 at high temperatures the decomposition of Na_2O can cause a weight loss and lead to an inhomogeneous compound. During growth a white powder of Na_2O is observed to volatilize and deposit on the inner wall of the quartz tube. By weighing a total weight loss ≈6 wt% is estimated. This value is in agreement with the data shown in Fig. 1(b), neglecting the tiny loss of oxygen caused by the change of cobalt valence state. The main loss of Na_2O is found during the premelting procedure, estimated to be ≈5 wt%. This is probably caused by incompletely reacted Na_2O when the mixtures are calcined and sintered prior to premelting. An additional ≈1 wt% loss is estimated after the crystal growth.

During growth, we observed that the molten zone is rather stable and Na_xCoO_2 single crystals with a sodium content of $x = 0.70$–0.90 are easily formed. In contrast, it is hard to grow the compound with $x = 0.50$–0.60. The analysis of EDX indicates that as-grown Na_xCoO_2 with $x < 0.6$ consists of multiphases like Na_2O and CoO_2 and Na-poor phases.

Large and high quality single crystals were obtained with a growth rate of ≈2 mm/h in flowing oxygen atmosphere. Figure 2 shows a typical crystal ingot of $Na_{0.7}CoO_2$. The *00l* face is readily cleaved mechanically due to the layered structure of the compound. Figure 3(a) displays one-half of the crystal platelets with the *00l* face of several cm^2 area cleaved from an ingot with a sharp scalpel. Figure 3(b) shows the other half after water intercalation. Crystal grains are found

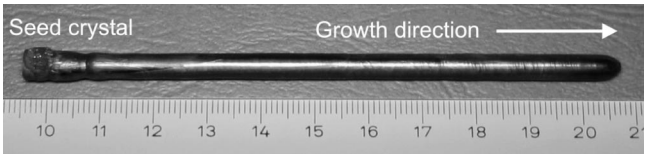

FIG. 2. A typical $Na_{0.7}CoO_2$ single-crystal ingot obtained by the optical floating zone technique.

to grow preferably along the *a* crystallographic axis, parallel to the rod axis.

A convex growth interface is observed to be the boundary between the regions of smaller and larger diameter of the crystal ingot, as shown in Fig. 3. The smaller one is formed when the molten zone was at lower temperatures and the larger one is formed at higher temperatures. Therefore the unequal diameter for an ingot indicates that temperature fluctuations occurred at the molten zone during growth. According to the temperature-composition relationship a fluctuation of heating temperature may result in a composition change of the molten zone, leading to an inhomogeneous compound. Figure 3(a) shows that many tiny crystal grains of CoO_2 gather at the boundary of the growth front. These grains can be removed after the deintercalation treatment, as shown in Figs. 3(b) and 3(c), respectively. It is important to maintain a stable molten zone by applying a constant heating temperature for growing a high quality single crystal.

Single-crystal XRD powder diffraction of $Na_{0.7}CoO_2$ gives the following lattice parameters and cell volume of the space group $P63/mmc$: $a=2.8278(4)$ Å, $c=10.9073(0)$ Å, $v=75.54$ Å.[3] Sintered powders show slightly different XRD patterns with $a=2.8230(2)$ Å, $c=10.9628(8)$ Å.[1]

For the determination of Na/Co compositions using EDX the crystal was scanned through a 3 mm segment along the growth direction taking the average of four measured points

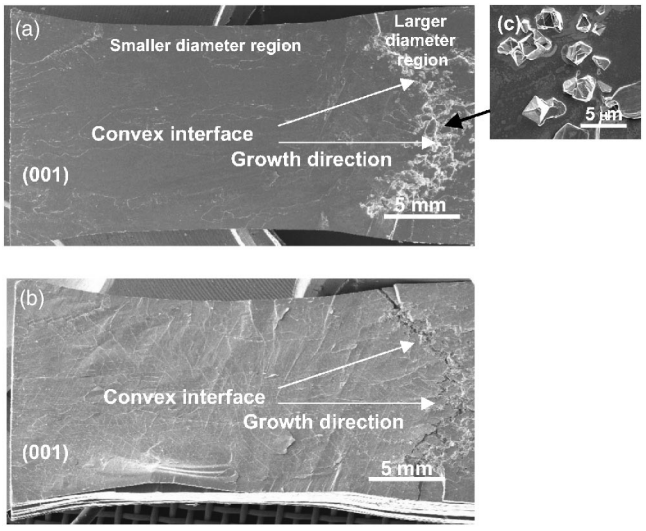

FIG. 3. Two halves of an as-grown crystal ingot with the 001 surface. (a) The as-cleaved half $Na_{0.7}CoO_2$ showing the CoO_2 inclusions gathering at the growth boundary and (b) the other half $Na_{0.3}CoO_2 \cdot yH_2O$ showing the removal of the CoO_2 inclusions after deintercalation followed by hydration. (c) The enlarged CoO_2 inclusions.

in the central and edge region of the crystal. It is found that the Na content varied with the temperature fluctuations during growth. At the beginning of the growth the temperature fluctuations are high and cause a high variation of the composition, $\Delta x \approx 0.11$, determined within 2 cm from the seeding part of the ingot. Following the seeding part the variation of Na content is smaller, $\Delta x \approx 0.06$, when the molten zone is maintained in a stable state by a constant temperature. A volatilized white Na_2O powder accumulates on the inner wall of the quartz tube after the growth is completed. The loss of Na may result in a reduction of its concentration in the as-grown crystal. The white Na_2O powders also form on the surface of crystals if the samples are stored under ambient conditions. Therefore the grown crystals must be stored in an evacuated container or a desiccator to avoid decomposition.

C. Sodium extraction and water intercalation

The superconducting phase $Na_xCoO_2 \cdot yH_2O$ ($0.26 \leqslant x \leqslant 0.42, y \approx 1.3$) is obtained by chemically extracting (deintercalation) sodium from Na_xCoO_2, followed by hydration. Single crystals of $Na_{0.7}CoO_2$ were placed in the oxidizing agent Br_2/CH_3CN for around 100 h and then washed with acetonitrile. The change of sodium content of the resulting crystals is generally proportional to the bromine concentration in the CH_3CN agent.[3] A crystal of Na_xCoO_2 with $x=0.3$ can result from a 6.6 mol Br_2/CH_3CN treatment only after a long extraction time of more than 1 week. The Na extraction of the compound was also carried out by the electrochemical method. The composition $Na_{0.3}CoO_2$ could be achieved in aqueous solution of NaOH using a constant current of 0.5 mA and a voltage of 1.0 V for over 10 days. Comparing the published 1–5 days extraction time for the $Na_{0.7}CoO_2$ powders[1,3] the crystal needs longer time to complete the extraction, also depending on the dimension of the sample. The slower extraction reaction in single crystals compared to a powder is related to the higher perfection and longer period of Na–O–Na within the NaO layers. In powder samples variations of the bonding are expected on a nanometer scale. Before and after the extraction treatment the sodium composition distribution across the crystals was determined by EDX.

The superconducting phase is then obtained by immersing the deintercalated samples for a week in H_2O/D_2O, or sealing the samples in a water vapor saturated container at room temperature. After hydration/deuteration a large increase in thickness is visible to the naked eyes and the morphology exhibits "booklet"-like layered cracks perpendicular to the *c* axis. The sodium intercalant layer expands with decreasing Na content because the Na removal results in Co oxidation (Co^{3+} ions oxidized to smaller Co^{4+} ions) and thus the CoO_2 layers are expected to shrink.[1,2] This suggests that a decreased bonding interaction between layers with decreasing Na content may result in a readily cleaving plane. Figures 4(a) and 4(b) illustrate the layered structures of the nonhydrated and fully hydrated phases of the compound, respectively. According to the layered structure of Na_xCo_2,[17] 24 Co–O bonds in the layer of CoO_2 form an octahedral CoO_6

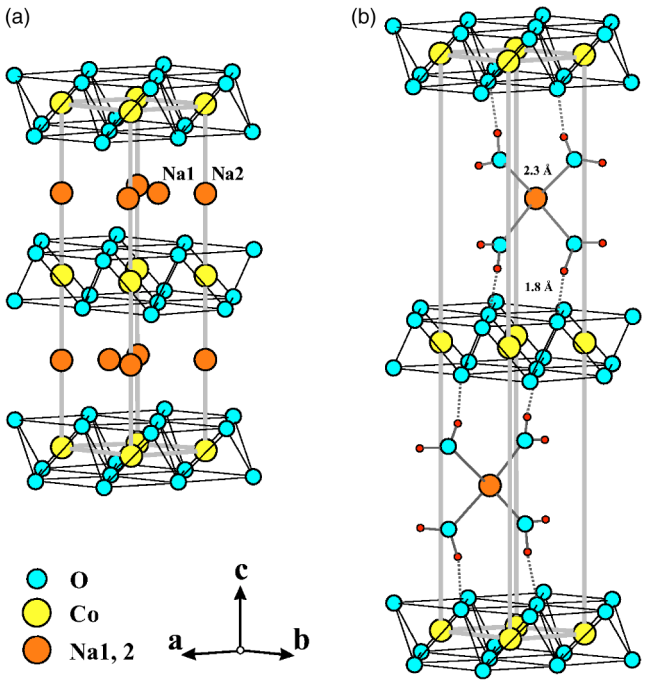

FIG. 4. Schematic drawing of the layered structures Ref. 17 for (a) nonhydrated $Na_{0.61}CoO_2$ and (b) fully hydrated $Na_{0.33}CoO_2 1.3H_2O$.

with high bonding energy and therefore the layer is structurally robust, while the bonding energy is much weaker in the NaO layer because the Na^+ mobility is high and the number of bonds Na 1–O is 6 and Na 2–O only 4/3. Therefore the Na layer readily collapses to leave the CoO_2 layer terminated as the outermost surface of the crystal. Moreover, the insertion of water induces two additional intercalated layers of H_2O between NaO and CoO_2, i.e., from Co–Na–Co to Co–H_2O–Na–H_2O–Na–Co, which results in the expansion of the *c* lattice constant from 11.2 to 19.6 Å. The hydrogen in the new intercalated H_2O layer bonds extremely weakly to the NaO and CoO layers. Therefore this compound is exceptionally unstable with respect to a change of thermal, mechanical, or humidity environment. Under ambient, oxidizing, and humid conditions the crystal exhibits three typical morphologies, as shown in Figs. 5(a)–5(c), respectively.

D. Behavior of the crystals upon hydration and dehydration

To study the phase formation and problems with rehydration we have performed detailed x-ray diffraction experiments as a function of time. Single crystals of nonhydrated $Na_{0.3}CoO_2$ have been partially hydrated in humid air to form $Na_{0.3}CoO_2 0.6H_2O$ under ambient conditions. These crystals were immersed in water with the *c* surface exposed to air. Each measurement of the 002 reflections was carried out for a short time of ≈3 min to avoid the x-ray that emits off the sample surface due to the rapid expansion of crystal thickness during the hydrating process. We show in Fig. 6 that the increase of intensity of the *002* reflection (corresponding to $y=1.3$) is accompanied by a decrease of intensity of the other two *002* reflections (corresponding to $y=0.6$ and 0, respectively). This is indicative of the increase of the volume of hydrated phase $y=1.3$ while decreasing the nonhydrated and partial hydrate phases, $y=0$ and 0.6. After a 1 day hydration the sample becomes completely "wet." This is indicated by the 002 reflections for the $y=1.3$ and 0.6 phases and the disappearance of the 002 corresponding to the nonhydrated phase $y=0$. Note that the 002 reflection of the partial hydrate with $y=0.6$ still exists until a further hydration up to 10 days. In the meantime the XRD pattern shows a continuously increasing volume fraction of the $y=1.3$ phase reaching approximately 100%. This suggests that the initial hydration process takes place with two water molecules per formula unit (corresponding to $y=0.6$) inserted into the Na plane, and followed by a group of four (corresponding to $y=1.3$) to form clusters of $Na(H_2O_4)$.

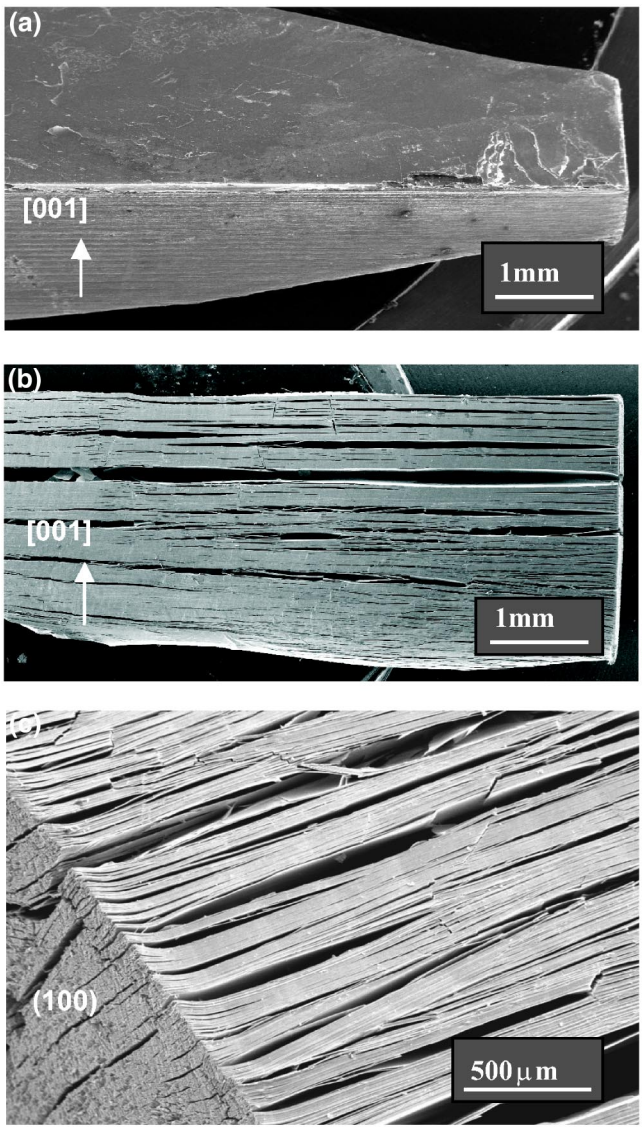

FIG. 5. Three typical morphologies showing the layered structure of Na_xCoO_2 single crystal. (a) After cutting an as-grown $Na_{0.7}CoO_2$ single crystal, (b) the cracked layers perpendicular to the c axis of the $Na_{0.3}CoO_2$ crystals after deintercalation, and (c) the "booklet"-like structure of the $Na_{0.3}CoO_2 1.3H_2O$ after being hydrated by H_2O.

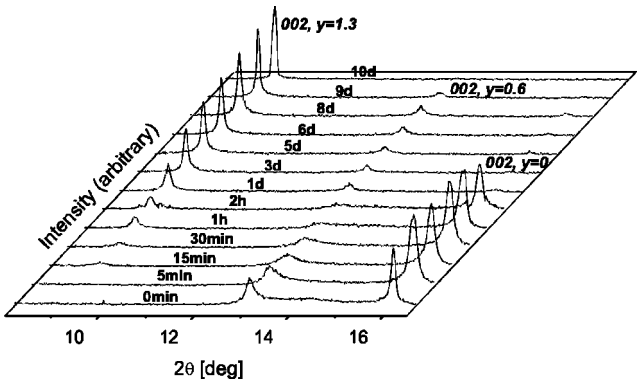

FIG. 6. Single crystal x-ray diffraction patterns for $Na_{0.3}CoO_2 \cdot yH_2O$ measured by immersing the sample in deionized water. The initial crystal contained the phases of $y=0.6$ and 0.

The hydrated volume of a crystal is a function of hydration time since the water diffuses gradually in the *ab* plane whereas the *c* face is robust and no diffusion path exists along the *c* axis. A fully hydrated phase $y=1.3$, exhibiting superconductivity, is achieved after 10 days for a crystal of 2×2 mm^2 in the a/b direction, concomitant with the disappearance of the partial hydrates of the other two *002* reflections, as shown in Fig. 6. This indicates that the phase $y=1.3$ is formed with four water molecules (two above and two below) to each Na ion when a longer diffusion time is allowed for creating a water-saturated environment during the hydration process.

A thermogravimetric analysis can be used to monitor the loss of water and stability of the hydrated phases as a function of temperature and time. Figure 7 shows the temperature dependence of water loss for an overhydrated sample ($y=1.8$) under a slow heating rate of 0.3°C/min in flowing oxygen. The fastest loss of water occurs between 20 and 50°C and is then again increasing upon further heating. The sample weight is characterized by several relatively broad plateaus in weight that are attributed to phases with $y=1.8$, 0.9, 0.6, 0.3, and 0.1 for temperatures near 28, 50, 100, 200, and 300°C, respectively. These data suggest the existence of the following majority phases at the respective temperatures: $Na_{0.3}CoO_2 1.8H_2O$($c=22.38$ Å), $Na_{0.3}CoO_2 0.9H_2O$($c=13.85$ Å), $Na_{0.3}CoO_2 0.6H_2O$($c=13.82$ Å), $Na_{0.3}CoO_2 0.3H_2O$($c=12.49$ Å), and $Na_{0.3}CoO_2 0.1\ H_2O$($c=11.20$ Å). A change of $\Delta y=0.33$ corresponds to the removal of one water molecule per formula unit. A complete removal of water ($y=0$) from the compound takes place at temperatures over 600°C.

Analysis of DTA-TG confirms that the fully hydrated superconducting phase ($y=1.3$) is rather unstable between 20 and 50°C due to the rapid loss of water. However, the superconducting phase can be reformed easily by rehydration. The inset of Fig. 7 shows the time dependence of the loss of water at room temperature. A rapid loss of water from $y=1.8$ to 0.6 occurs in 1.5 h and then no further weight loss is observed during 1 day. XRD reveals that the flat plateau corresponding to a semihydrated $Na_{0.3}CoO_2 0.6H_2O$ with $y=0.6$ appears to be a metastable phase under ambient conditions. This observation is in conflict with that for polycrystalline powders.[2]

The fact of the matter is that a single crystal is only one domain containing crystal water while powder samples consist of countless tiny grains with additional intergrain water. Furthermore, the loss or absorption of water in a large single crystal is slower and more well-defined compared to powders due to the diffusion path along the Na layer.

E. Mixture of cells

As shown in the TGA data, a fully hydrated sample can release water under ambient conditions to form partial hydrates. On the other hand, moisture from air can also be absorbed by a nonhydrated sample to form hydrated phases. In order to quantitatively identify the hydrated phases in the crystal, the fully hydrated or nonhydrated samples were placed in a humid or dry atmosphere. They were then inves-

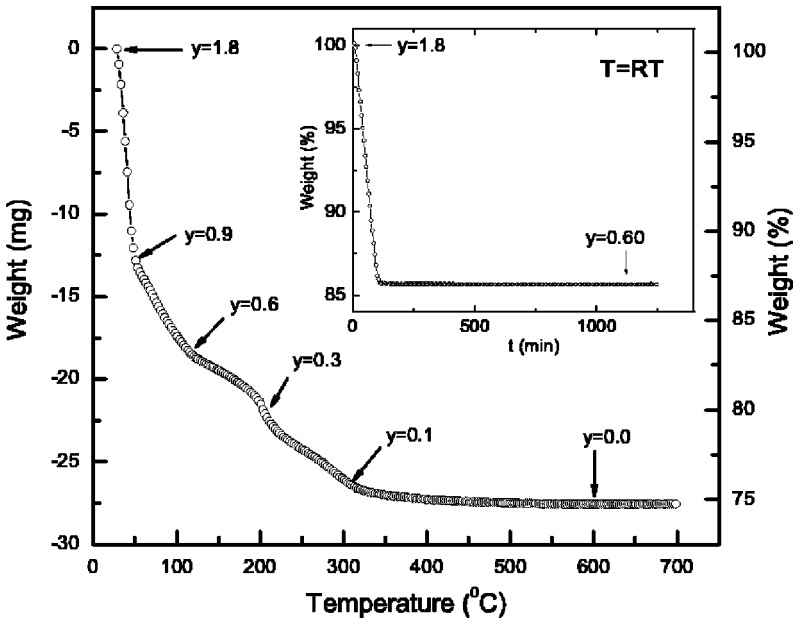

FIG. 7. Thermogravimetric analysis of an overhydrated $Na_{0.3}CoO_2 1.8H_2O$ single crystal heated at 0.3 K/min in flowing oxygen. Inset: time dependence of the weight loss for the same specimen at room temperature in flowing oxygen. Initial mass of the sample was 112.965 mg. The loss was approximately 19 mg after heating and rehydrating.

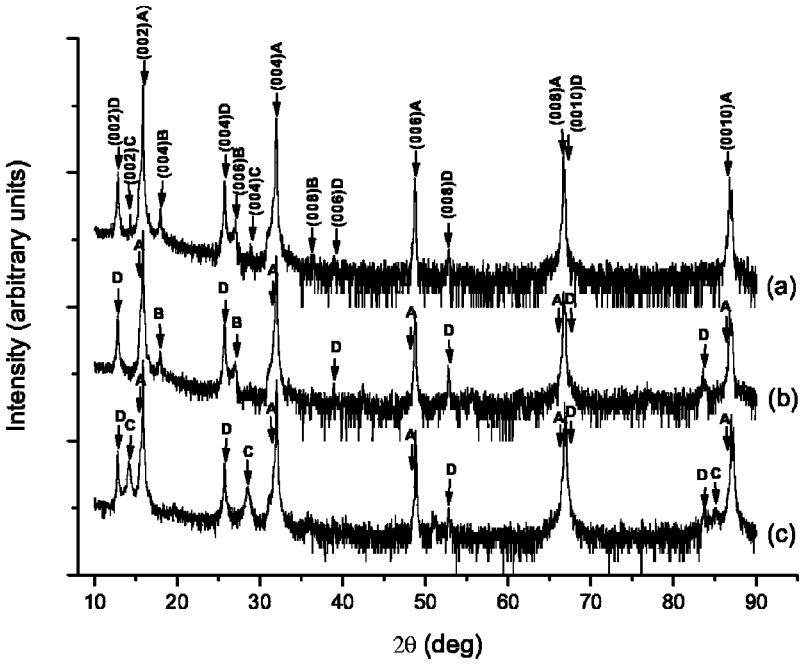

FIG. 8. The *00l* reflections showing the mixture of cells and the lattice constants for the various hydrates of $Na_{0.3}CoO_2 \cdot yH_2O$ under different ambient conditions. (a) From humid to dry air for 2 days, (b) from humid to dry air for 5 days, and (c) from dry to humid air for 5 days. Symbol **A** represents the phase of $y=0$ for $a=2.82$Å and $c=11.195$Å, **B**: $y=1.3$ for $a=2.82$Å and $c=19.710$Å, **C**: $y=0.3$ for $a=2.82$Å and $c=12.478$Å, and **D**: $y=0.6$ for $a=2.82$Å and $c=13.815$Å.

tigated by XRD and the results show a clear shift in the positions of the *00l* reflections for both samples, yielding several variations in the *c* axes of the unit cells, as shown in Figs. 8(a)–8(c). The fully hydrated phase of $Na_{0.3}CoO_2 1.3H_2O$ is exposed to dry air at ambient conditions for 2 and 5 days, resulting in the formation of four and three mixed phases, as shown in Figs. 8(a) and 8(b), respectively. Exposing a nonhydrated $Na_{0.3}CoO_2$ to humid air for 5 days results in two additional phases of $Na_{0.3}CoO_2 0.3H_2O$ and $Na_{0.3}CoO_2 0.6H_2O$, as shown in Fig. 8(c). Note that the phase with $y=0.6$ is always observed in the crystals under ambient conditions. Nevertheless, to prevent a fully hydrated phase from losing water we suggest that the samples be stored in a saturated humid atmosphere. Nonhydrated samples can be stored in an evacuated container to prevent decomposition from absorbing water in air.

F. Electrical properties

We have performed transport experiments of the out-of-plane resistivity ρ_c as a function of time to further characterize the hydration dynamics. The initially nonhydrated single crystal $Na_{0.3}CoO_2$ was immersed in deionized water throughout the whole experiment. In contrast to measurements of powder samples in humid air, this configuration reduces the influence of internal and external surfaces and allows a full and continuous hydration. Furthermore, the out-of-plane resistivity ρ_c measured in four-point geometry should be less affected by the intrinsic Na ion conductivity.

In Fig. 9 and its inset plateaus and steps of the resistivity are given with increasing hydration time followed by a continuous and then more gradual decrease. Noteworthy is the similar resistivity reached after 8 h compared to the initial state. This implies that, although irreversible by nature, the

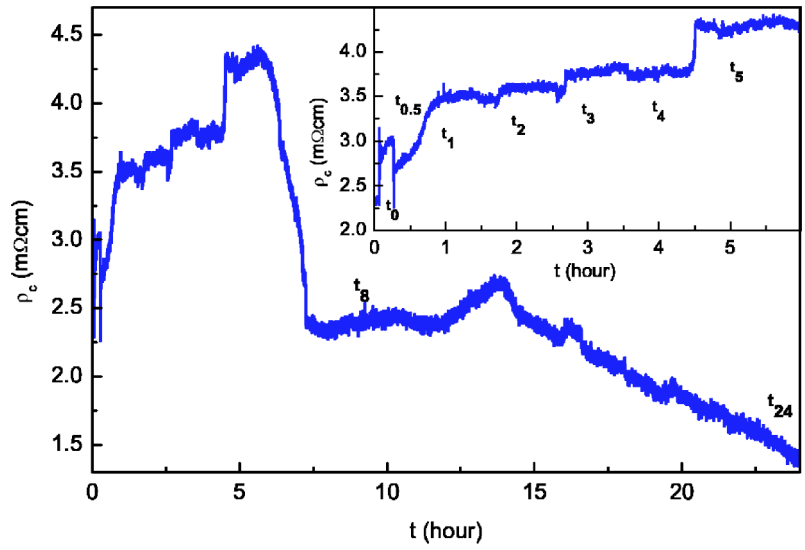

FIG. 9. Time dependence of the out-of-plane resistivity ρ_c of a $Na_{0.3}CoO_2 \cdot yH_2O$ single crystal during a hydration process. The number given as footnote at the plateaus is hydration time in hours.

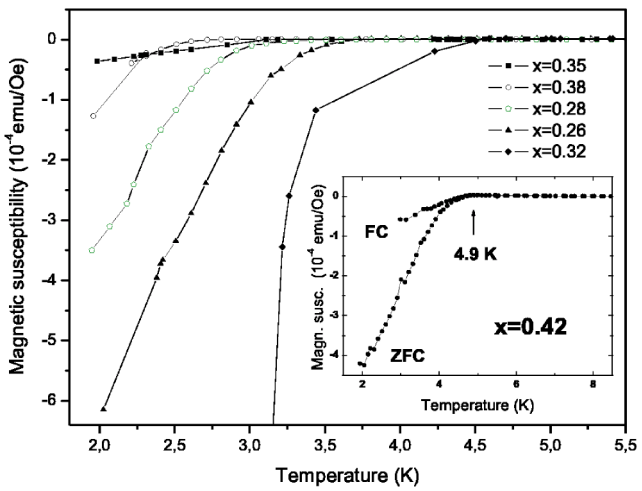

FIG. 10. Zero field Cooling (ZFC) magnetic characterization of the $Na_xCoO_21.3H_2O$ single crystals showing the onset $T_c(x)$. Inset: optimum $T_c \approx 4.9$ K with $x=0.42$ as ZFC and FC measurement.

hydration process has also reversible stages. During hydration the water molecules enter the compound to intercalate between the CoO_2 and Na layers. The CoO_2 layers are separated by a trilayer of $H_2O/Na/H_2O$. The dominant effect is to expand the *c*-axis lattice parameters, from about 11.2 Å without water (nonsuperconducting phase $Na_{0.3}CoO_2 \cdot yH_2O$, $y=0$) to 12.5 Å (semihydrated phase, $y=0.6$) and then to 19.5Å when the system becomes superconducting ($y=1.3$) (see Fig. 6). This is related to an enlarged interlayer distance from 5.6 to 6.9 Å and then to 9.8 Å. The stepwise increase from t_0 to t_5 occurs at a constant chemical doping level and suggests that the increase of spacing between the CoO_2 layers leads to the resistivity increase. We propose that the rapid steps followed by plateaus map the dynamics of domains of hydration that are pinned at the random potential of the local defect landscape. The more gradual decrease of resistivity for $t>12$ hours must therefore be related to a more homogeneous state of the system.

There is an interesting correlation between the CoO_2 layer and the superconducting transition temperature, i.e., the Co–O distance decreases with increasing T_c.[17] The layer thickness of CoO_2 changes from 1.93 Å for the nonsuperconducting phase to 1.84 Å for the superconducting phase.[18] It is clear that the layer thickness of CoO_2 shrinks after reaching full hydration or doping to $y=1.3$ and a change in the oxidation state of Co occurs because the oxidation state directly corresponds to the carrier density in the CoO_2 layers and some electron transfer off the cobalt.[1] Recently, also a relation between the *c* axis parameter and the superconducting transition temperature has been discussed.[19] Nevertheless, the change of the room temperature resistivity during the hydration process is not only influenced by the expansion of spacing in the system but also by a redistribution of the charge in the CoO_2 layer.

G. Superconductivity

The superconducting properties of the fully hydrated single crystals were characterized by ac susceptibility using a superconducting quantum interference device magnetometer. Zero field cooling measurements with 10 Oe applied field are presented in Fig. 10. Superconducting transition temperatures $T_c=2.8-4.9$ K with $x\approx 0.28-0.42$ are observed, respectively. Some of our samples showed strong diamagnetic ac signals and a superconducting volume fraction as high as 20%. The transition width for each sample is different, which is very likely caused by an inhomogeneous sodium concentration and partial hydration that affect the superconducting state of $Na_xCoO_21.3H_2O$. The T_c values vary with Na content, showing the highest T_c at 4.9 K with $x=0.42$ given in the inset of Fig. 10. As shown in the inset the onset of the superconducting transition is identical with the divergence of FC and ZFC data.

Figure 11 is the plot of T_c as a function of sodium concentration of $Na_xCoO_21.3H_2O$. For samples with $x\leqslant 0.22$ and $x\geqslant 0.47$ there is no superconducting transition detectable. The open (closed) symbols correspond to the onset (low temperature extrapolated) transition temperatures. These data agree to some extent with a recent study that shows a constant T_c for Na contents up to 0.37.[19] However, they conflict with the superconducting "dome" of $T_c(x)$ demonstrated for powder samples.[3] This latter dependence motivated the proposal of intrinsic critical concentrations $x_{cr1}\approx 1/4$ and x_{cr2}

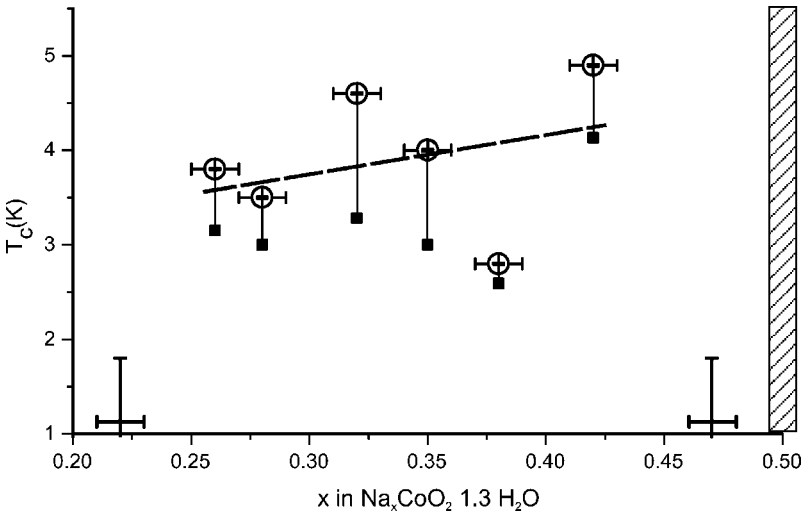

FIG. 11. Superconducting phase diagram as a function of Na content. Open circles correspond to the onset temperature, while closed square correspond to a linear low-temperatures extrapolation. The dashed line is a guide to the eye. The dashed bar marks the metal-insulator transition observed in nonhydrated $Na_{0.5}CoO_2$.

$\approx 1/3$ related to charge ordering instabilities of the Co^{3+}/Co^{4+}.[20] In the present single crystal study the upper limit is shifted to much higher concentrations, $x_{cr2} \approx 0.45$. This implies that a charge ordering at $x_{cr2} \approx 1/3$ is not relevant to suppress T_c.

However, the superconducting phase now extends close to the phase line where nonhydrated $Na_{0.5}CoO_2$ shows a metal-insulator transition.[10] This is evidence for an importance of electronic correlations at higher x in the hydrated system. It is interesting to note that the Néel transition $T_N \approx 20$ K is also only observed for higher Na concentrations $x > 0.75$ in nonhydrated crystals, and that this ordering temperature does not change appreciably with x. Bulk antiferromagnetic order has been proven using myon spin rotation and other thermodynamic experimental techniques.[6] The exact nature of the ordering, however, is still in need of further investigation.

Evidence for superlattice formation and electronic instabilities either due to Na or Co^{3+}/Co^{4+} charge ordering are recently accumulating for nonhydrated Na_xCoO_2 with $x = 0.5$, but also to some extent for other stoichiometries.[21,22] Hydration contributes to the charge redistribution due to its effect on the CoO_2 layer thickness and the formation of $Na(H_2O)_4$ clusters that shield disorder of the partially occupied Na sites. The above-mentioned instabilities should influence the superconducting state as they modulate the electronic density of states and change nesting properties of the Fermi surface.[8,9] Further studies are needed to investigate a possible interrelation of Na content, hydration, and structural details on well-characterized samples with the highest T_c.

IV. CONCLUSION

Using TG-DTA we found that Na_xCoO_2 is an incongruently melting compound, and single crystals can be grown using the optical floating zone technique. Both nonhydrated and fully hydrated crystals are exceptionally sensitive under ambient conditions. The study of XRD and TG indicates that the semihydrated phase $Na_xCoO_2 0.6H_2O$ is more stable than the other compositions under ambient conditions. The XRD patterns show the presence of cells corresponding to the coexistence of several different hydrated phases in rehydrated samples. The superconducting transition temperature of $Na_xCoO_2 1.3H_2O$ is only weakly influenced by the Na content. The highest $T_c \approx 4.9$ K is found for $x \approx 0.42$, i.e., in the proximity of a metal-insulator transition observed in the nonhydrated phase with $x = 0.5$. The hydrated compound is strongly unstable concerning its chemical, structural, and electrical properties. We therefore propose to carefully reinvestigate the recently claimed evidence for unconventional superconductivity on single crystals.

ACKNOWLEDGMENTS

We thank E. Brücher, G. Götz, E. Peters, and E. Winckler for technical support.

*Corresponding author. Email address: ct.lin@fkf.mpg.de

[1] K. Takada, H. Sakurai, E. Takayama-Muromachi, F. Izumi, R. Dilanian, and T. Sasaki, Nature (London) **422**, 53 (2003).
[2] M. L. Foo, R. E. Schaak, V. L. Miller, T. Klimczuk, N. S. Rogado, Y. Wang, G. C Lau, C. Craley, H. W. Zandbergen, N. P. Ong, and R. J. Cava, Solid State Commun. **127**, 33 (2003).
[3] R. E. Schaak, T. Klimczuk, M. L. Foo, and R. J. Cava, Nature (London) **424**, 527 (2003).
[4] T. Fujimoto, G. Q. Zheng, Y. Kitaoka, R. L. Meng, J. Cmaidalka, and C. W Chu, cond-mat/0307127.
[5] R. Jin, B. C. Sales, P. Khalifah, and D. Mandrus, Phys. Rev. Lett. **91**, 217001 (2003).
[6] S. Bayrakci, C. Bernhard, D. P. Chen, B. Keimer, P. Lemmens, C. T. Lin, C. Niedermayer, and J. Strempfer, Phys. Rev. B **69**, 100410 (2004), and references therein.
[7] P. Lemmens, V. Gnezdilov, N. N. Kovaleva, K. Y. Choi, H. Sakurai, E. Takayama-Muromachi, K. Takada, T. Sasaki, D. P. Chen, F. C. Chou, C. T. Lin, and B. Keimer, J. Phys.: Condens. Matter **16**, S857 (2004), and references therein.
[8] A. Tanaka and X. Hu, Phys. Rev. Lett. **91**, 257006 (2003).
[9] M. D. Johannes, I. I. Mazin, D. J. Singh, and D. A. Papaconstantopolus, cond-mat/0403135.
[10] Q. Huang, M. L. Foo, J. W. Lynn, H. W. Zandbergen, G. Lawes, Y. Wang, B. H. Toby, A. P. Ramirez, N. P. Ong, and R. J. Cava, cond-mat/0402255.
[11] F. Rivadulla, J.-S. Zhou, and J. B. Goodenough, Phys. Rev. B **68**, 075108 (2003).
[12] T. Motohashi, E. Naujalis, R. Ueda, K. Isawa, M. Karppinen, and H. Yamauchi, Appl. Phys. Lett. **79**, 1480 (2001).
[13] K. Fujita, T. Mochida, and K. Nakamura, Jpn. J. Appl. Phys., Part 1 **40**, 4644 (2001).
[14] F. C. Chou, J. H. Cho, P. A. Lee, E. T. Abel, K. Matan, and Y. S. Lee, Phys. Rev. Lett. **92**, 157004 (2004).
[15] M. Chen, B. Hallstedt, and L. J. Gauckler, J. Phase Equilib. **24**, 212 (2003).
[16] H. A. Wriedt, Bull. Alloy Phase Diagrams **8**, 234 (1987).
[17] J. D. Jorgensen, M. Avdeev, D. G. Hinks, J. C. Burley, and S. Short, Phys. Rev. B **68**, 214517 (2003).
[18] J. W. Lynn, Q. Huang, C. M. Brown, V. L. Miller, M. L. Foo, R. E. Schaak, C. Y. Jones, E. A. Mackey, and R. J. Cava, Phys. Rev. B **68**, 214516 (2003).
[19] C. J. Milne, D. N. Argyriou, A. Chemseddine, N. Aliouane, J. Veira, and D. Alber, cond-mat/0401273.
[20] G. Baskaran, cond-mat/0306569.
[21] H. W. Zandbergen, M. L. Foo, Q. Xu, V. Kumar, and R. J. Cava, cond-mat/0403206.
[22] J. L. Gavilano, D. Rau, B. Pedrini, J. Hinderer, H. R. Ott, S. M. Kazakov, and J. Karpinski, Phys. Rev. B **69**, 100404(R) (2004).